FULL PAPER

Remote triggering of seismicity at Japanese volcanoes following the 2016 M7.3 Kumamoto earthquake

Bogdan Enescu[1*] , Kengo Shimojo[2], Anca Opris[2] and Yuji Yagi[3]

Abstract

The M_{JMA}7.3 Kumamoto earthquake occurred on April 16, 2016, in the western part of Kyushu, at a depth of 12 km, on an active strike-slip fault. Here, we report on a relatively widespread activation of small remote earthquakes, which occurred as far as Hokkaido, detected by analyzing the continuous waveform data recorded at seismic stations all over Japan. Such relatively widespread remote seismicity activation, following a large inland earthquake, has not been reported before for Japan. Our analysis demonstrates that the remote events were triggered dynamically, by the passage of the surface waves from the Kumamoto earthquake. Most of the remotely triggered events in the Tohoku and Hokkaido regions, as well as close to Izu Peninsula, occur at or close to volcanoes, which suggests that the excitation of crustal fluids, by the passage of Rayleigh waves, played an important triggering role. Nevertheless, remote activation in other regions, like Noto Peninsula, occurred away from volcanoes. The relatively large-amplitude Love waves, enhanced by a source directivity effect during the Kumamoto earthquake, may have triggered seismicity on local active faults. The dynamic stresses in the areas where remote activation has been observed range from several kPa to tens of kPa, the thresholds being lower than in previous dynamic triggering cases for Japan; this might relate to a change in the crustal conditions following the 2011 M9.0 Tohoku-oki earthquake, in particular at volcanoes in NE Japan.

Keywords: Kumamoto earthquake, Remote triggering, Volcanoes, Active faults, Dynamic stresses

Background

Activation of seismicity at remote locations due to the passage of seismic waves from relatively large earthquakes is a well-documented phenomenon (e.g., Hill et al. 1993; Brodsky et al. 2000), although the responsible underlying physical processes are still under debate (e.g., Hill and Prejean 2015).

The static stress changes decay with distance, *r*, approximately proportional to r^{-3}, for distances exceeding the source extent (Aki and Richards 2002), while the dynamic stress changes (due to the passage of surface waves) attenuate much slower (as $r^{-3/2}$, for surface waves, Hill et al. 1993). Therefore, in general, activated seismicity

that occurs at more than a few lengths from the mainshock could be attributed to dynamic rather than static stress changes, since the last ones become negligible. The shaking produced by the surface waves at a certain location depends not only on the distance between the source and receiver, but also on other factors such as directivity, radiation pattern and crustal structure (e.g., Manga and Brodsky 2006). Nevertheless, the significant difference in dependence on distance is a robust feature to distinguish static and dynamic stress triggering (e.g., Manga and Brodsky, 2006).

The physical mechanisms that operate to trigger earthquakes remotely are still under debate. Nevertheless, two main classes of models (Hill and Prejean 2015) are used to explain the triggering by dynamic stresses: (1) direct triggering by frictional failure and (2) triggering through excitation of crustal fluids. As documented in previous studies (e.g., Aiken and Peng 2014), fluids are active

---

*Correspondence: benescu@kugi.kyoto-u.ac.jp
[1] Department of Geophysics, Faculty of Science, Kyoto University, Kita-Shirakawa, Oiwake-cho, Sakyo-ku, Kyoto 606-8502, Japan
Full list of author information is available at the end of the article

Enescu *et al. Earth, Planets and Space* (2016) 68:165

Page 2 of 9

agents in geothermal and volcanic areas, where dynamic triggering is often observed.

Somewhat surprisingly, Harrington and Brodsky (2006) report a relative lack of remotely triggered seismicity in Japan and propose some qualitative models to explain their observations. They find, however, that Kyushu (characterized by extensional tectonics and intense volcanism) shows some limited triggering following teleseismic events. Parsons et al. (2014) found as well that Japan has a relatively low triggering potential compared with other seismotectonic regions.

Recently, Miyazawa (2011) showed that extensive remote triggering of seismicity in Japan followed the occurrence of the 2011 M9.0 Tohoku-oki earthquake, at regions as far as Kyushu, at more than 1300 km distance from the Tohoku-oki epicenter. Since at such large distances the effect of static stress changes due to the mainshock is negligible and, in addition, the remote activations of seismicity followed the propagation of surface waves from the Tohoku-oki earthquake, Miyazawa (2011) concluded that the remote activation occurred due to changes in dynamic stress accompanying the passage of surface waves from the M9.0 earthquake.

Thus, with the notable exception of the 2011 Tohoku-oki earthquake (e.g., Miyazawa 2011; Yukutake et al. 2011), remote triggering in Japan seems scarce at least (e.g., Harrington and Brodsky 2006).

In this study, we report on a relatively widespread activation of remote seismicity following the 2016 M7.3 Kumamoto earthquake, which occurred on the active strike-slip Futagawa fault, in the western part of Kyushu Island, Japan, at relatively shallow depth (12 km). We show that the seismic activity is triggered dynamically, in particular at or close to volcanoes, and speculate on the mechanism that may explain these observations. Our study is motivated by the size of the 2016 Kumamoto earthquake, which is the largest inland event (M7.3) occurred in Japan after the 2011 Tohoku-oki earthquake; we considered the occurrence of this earthquake an excellent opportunity to search for remote dynamic triggering in Japan.

Methods

We have processed waveform data recorded at high-sensitivity Hi-net and broadband F-net stations, operated by the National Institute for Earth Science and Disaster Resilience (NIED), as well as Japan Meteorological Agency (JMA) stations located at volcanoes throughout Japan. Moreover, we have also processed waveform data recorded by the V-net network, operated by NIED, at Japanese volcanoes. In total, we have downloaded and processed the continuous waveform data at more than 1000 seismic stations all over Japan.

We have first downloaded waveform data recorded within one hour before and after the mainshock occurrence time (March 16, 2016; 01:25:05, Japan standard time) and corrected adequately for instrument response.

In order to detect locally triggered events, we use a two-way Butterworth band-pass filter in the frequency range of 10–30 Hz. As we have experimented before (Shimojo et al. 2014), such a filtering ensures good detection of locally triggered remote events, while avoiding at least in part high-frequency noise. In many cases, the remote detections were confirmed by identifying the P- and S-wave arrival times of the triggered events.

In order to correlate the observed remote triggering with the passage of surface waves from the Kumamoto earthquake, we have used F-net and Hi-net data in the frequency range of 0.01–0.2 Hz (5–100 s). In this respect, the Hi-net data were processed using the approach of Maeda et al. (2011), who showed that the Hi-net waveforms can be successfully used to retrieve long-period ground motions after applying an appropriately designed recursive filter.

We have also used the JMA earthquake catalog to check the seismicity at the remotely triggered sites.

Results and discussion

Remote events triggered during the passage of Kumamoto earthquake surface waves

We show in Fig. 1 the location of seismic stations where remote earthquake triggering has been detected following the 2016 Kumamoto earthquake. The P-wave and S-wave arrivals of locally triggered events have been confirmed for most of the stations plotted in the figure. Stations where we could not be sure on the P- and S-wave arrivals, due to a rather poor signal-to-noise ratio (S/N), are shown in light colors. The S/N for the unambiguous wave arrivals had a median of 7.5 and minimum of 1.6 (smaller values were considered unreliable after careful visual inspection of seismograms). We have also eliminated, after visual inspection, spike-like signals that were considered to be noise rather than locally triggered events. In addition, stations located in areas where the "background seismicity" was masking the correlation of local seismicity with the passage of the mainshock surface waves were not considered in the analysis. In other words, all the selected cases correspond to visually sharp seismicity activations (at rates at least few times higher than the background). The (S-P) time is up to a few seconds for most of the remote events, which confirms that they occur in the vicinity of the seismic stations where the detection was made. We present in Additional file 1: Figure S1 a map similar to that of Fig. 1, which additionally shows Hi-net stations at which no earthquake triggering is observed. Many of the stations in southwest

Enescu *et al. Earth, Planets and Space* (2016) 68:165

Page 3 of 9
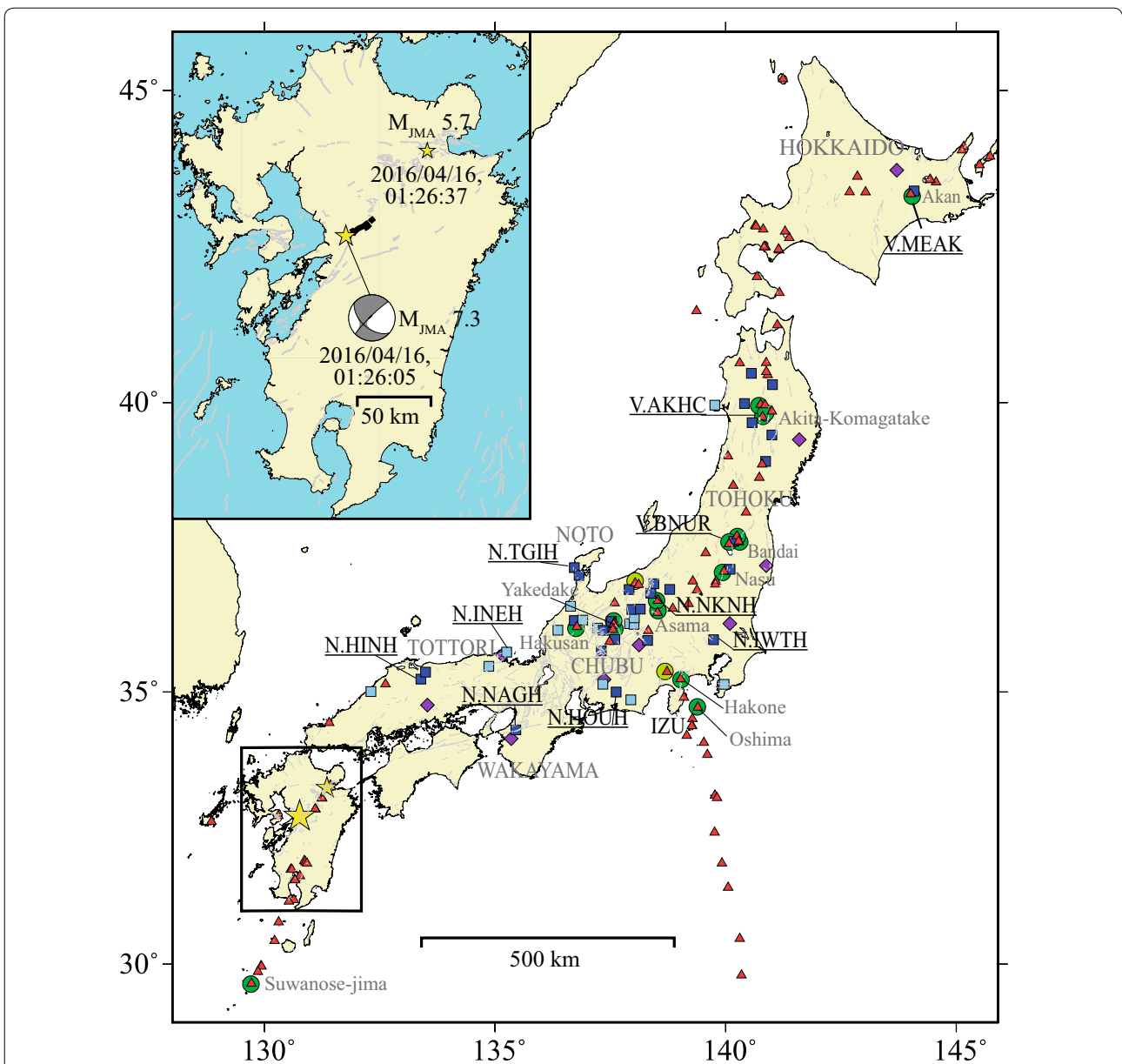
Fig. 1 Map showing the seismic stations where remote triggering has been observed after the Kumamoto earthquake. The stations of JMA network located at Quaternary active volcanoes are plotted as *green circles*, while the Hi-net (NIED) seismic stations are plotted as *blue rectangles*. *Lighter colors* indicate stations where the remote triggering occurred with less confidence (see text for additional explanations). The F-net stations used in Fig. 2b are shown as *purple diamonds*. Stations with names written nearby, belonging to the Hi-net and JMA networks, are those used in Figs. 2a and 3. The *red triangles* and *gray lines* indicate volcanoes and active faults, respectively. The name of some regions in Japan is indicated in *gray, uppercase letters*; the name of volcanoes close to which remote earthquake triggering has been observed is also indicated (*gray letters*). The two *yellow stars* (in the map and inset) indicate the M7.3 earthquake, and one of its immediate larger aftershocks in Oita prefecture occurred toward NE. The inset indicates the mechanism of the mainshock (F-net, NIED), its occurrence time and magnitude, as well as its source fault

Japan, where there are only few active volcanoes, do not show any triggered signal, although they are located relatively close to the mainshock hypocenter and the shaking there is relatively strong.

The closest "triggered" stations are located at about 300 km from the epicenter of the Kumamoto earthquake.

Since the length of the mainshock fault (Yagi et al. 2016) is of about 30–40 km, the static stress changes that operate at distances more than 7 times the fault length are too small to trigger seismicity. For example, in the case of the M7.4 Landers earthquake, the maximum stress changes calculated at epicentral distances more than ~4 times the

Enescu *et al. Earth, Planets and Space* (2016) 68:165

Page 4 of 9

fault-length drop below ~1–3 kPa (Hill et al. 1993); such values are much smaller than the dynamic stress changes at similar distances. We can therefore be confident that the triggering observed at the stations plotted in Fig. 1 is caused by dynamic rather than static stress changes.

The furthest triggered event was observed in Hokkaido, at about 1650 km epicentral distance, close to Akan volcano. Triggering has also been observed at (or close to) other volcanoes in Tohoku (Akita-Komatagatake, Bandai and Nasu volcanoes), Chubu (Yakedake, Asama and Hakusan volcanoes), close to Izu Peninsula (Hakone and Oshima volcanoes) and in the southern part of Kyushu (at the Suwanose-jima volcano). The seismicity at Hakone volcano (close to Izu Peninsula) has also been remotely activated following the 2011 Tohoku-oki earthquake (Yukutake et al. 2011), but no other remote triggering has been reported there so far, following other teleseismic events. Seismicity close to some volcanoes in Chubu (e.g., Hakusan and Yakedake volcano) was triggered dynamically following the 2011 megathrust event (Fig. 1 of Miyazawa 2011).

While remote seismicity triggering at volcanoes seems predominant, other regions of triggering include Wakayama, Tottori and Noto Peninsula, which correspond to active fault areas (and no volcanic activity).

Further support for the dynamic character of the triggered seismicity comes from Fig. 2. Figure 2a shows the high-frequency (10–30 Hz) filtered waveforms recorded at selected, but representative stations in Fig. 1. The gray reverse triangles show the approximate arrival time of Rayleigh waves assuming a nominal, typical phase velocity of 3.5 km/s (e.g., Aiken et al. 2013). Remotely triggered events can be identified as sudden increases of the high-frequency waveform amplitudes occurring at progressively later times, function of epicentral distance.

Figure 2b shows the low-frequency vertical seismograms (0.01–0.2 Hz) recorded at broadband F-net stations (Fig. 1). These F-net stations were the closest available from the Hi-net stations used in Fig. 2a. The gray circles indicate events identified on the high-frequency seismograms in Fig. 2a. Note that these events are plotted at the same epicentral distances as the recording Hi-net stations, at times corresponding to their P-wave arrival at the corresponding station. Since the (S-P) times of the detected events are mostly up to about 3 s (usually 1–2 s), the distance-related uncertainties are up to ~25 km. Most of the detected remote events occur only during the larger surface wave (Rayleigh) phases, but in some cases (station N.NKNH, Fig. 2a) the activation continues for longer times.

As one can notice in Fig. 2b, there is a good agreement between the arrival of surface waves (Rayleigh waves) from the Kumamoto earthquake and the

remotely triggered events. It is hard, however, to judge whether Rayleigh waves or Love waves (that can be identified on transverse-component, low-frequency seismograms—figure not shown) or both are responsible for the triggering. More insight can be gained from the detailed analysis of some triggering cases (Fig. 3), which were selected at increasingly larger distances from the mainshock.

In Fig. 3a, b and c, we present cases of remote triggering for three geographically different areas. The first and closest selected area is in Noto Peninsula, at ~750 km distance from the Kumamoto earthquake epicenter. We show in Fig. 3a the low-frequency (0.01–0.2 Hz) waveforms recorded at the Hi-net station N.AMZH ("N." is omitted in the figure and text below, for brevity) for the vertical, radial and transverse components. Waveforms are time-shifted to the epicenter of the triggered event, assumed to have occurred at the TGIH station location. The high-frequency (10–30 Hz) vertical-component waveform at TGIH station (location in Fig. 1) is also plotted. Note that the NS component at the TGIH station was not working at the time of the Kumamoto earthquake; therefore, we had to choose a nearby station (AMZH) for plotting the low-frequency seismograms. The plot at the bottom of the figure indicates clear P- and S-wave arrivals for one of the remotely triggered Noto events. The (S-P) time is of ~1.3 s, which indicates that the epicenter of the triggered event locates in the immediate vicinity of TGIH. The remote events clearly occur during the maximum phases of both the Love (transverse velocity component) and Rayleigh waves (vertical and radial velocity waveform components); however, it is difficult to judge which of the two is mostly responsible for the triggering. The remote triggering in Noto occurred likely on an active fault, close to the epicenter of a past large earthquake, the 2007 M6.9 Noto earthquake (e.g., Asano and Iwata 2011).
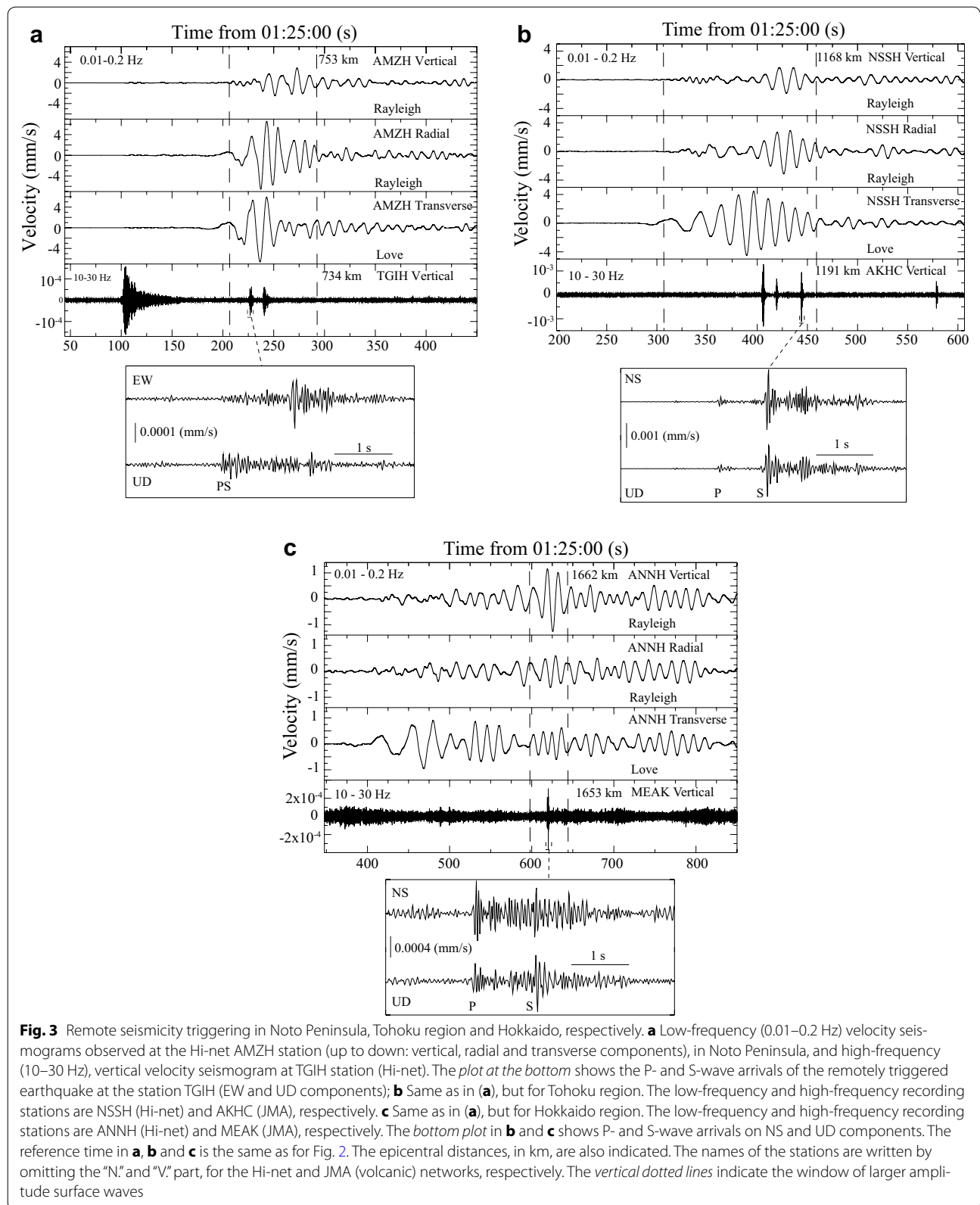
Figure 3b shows the triggering close to the Akita-Komagatake volcano (epicentral distance of 1168 km from the mainshock), which is one of the active volcanoes in northern Honshu. In a similar way with Fig. 3a, the triggered events occur during the passage of surface-wave phases from the Kumamoto earthquake. Since the (S-P) arrival times are of ~1 s (see bottom plot), we assume the location of the triggered events to be the same as the location of the AKHC station. The three triggered events (time window of 400–450 s) occur during largest amplitude Rayleigh and Love wave trains. However, there is some delay between the onset of the large-amplitude Love waves and the remotely triggered seismicity. This may be explained by either a relative lack of triggering efficiency of Love waves or some period-dependent triggering potential.

Enescu *et al. Earth, Planets and Space* (2016) 68:165

Page 5 of 9
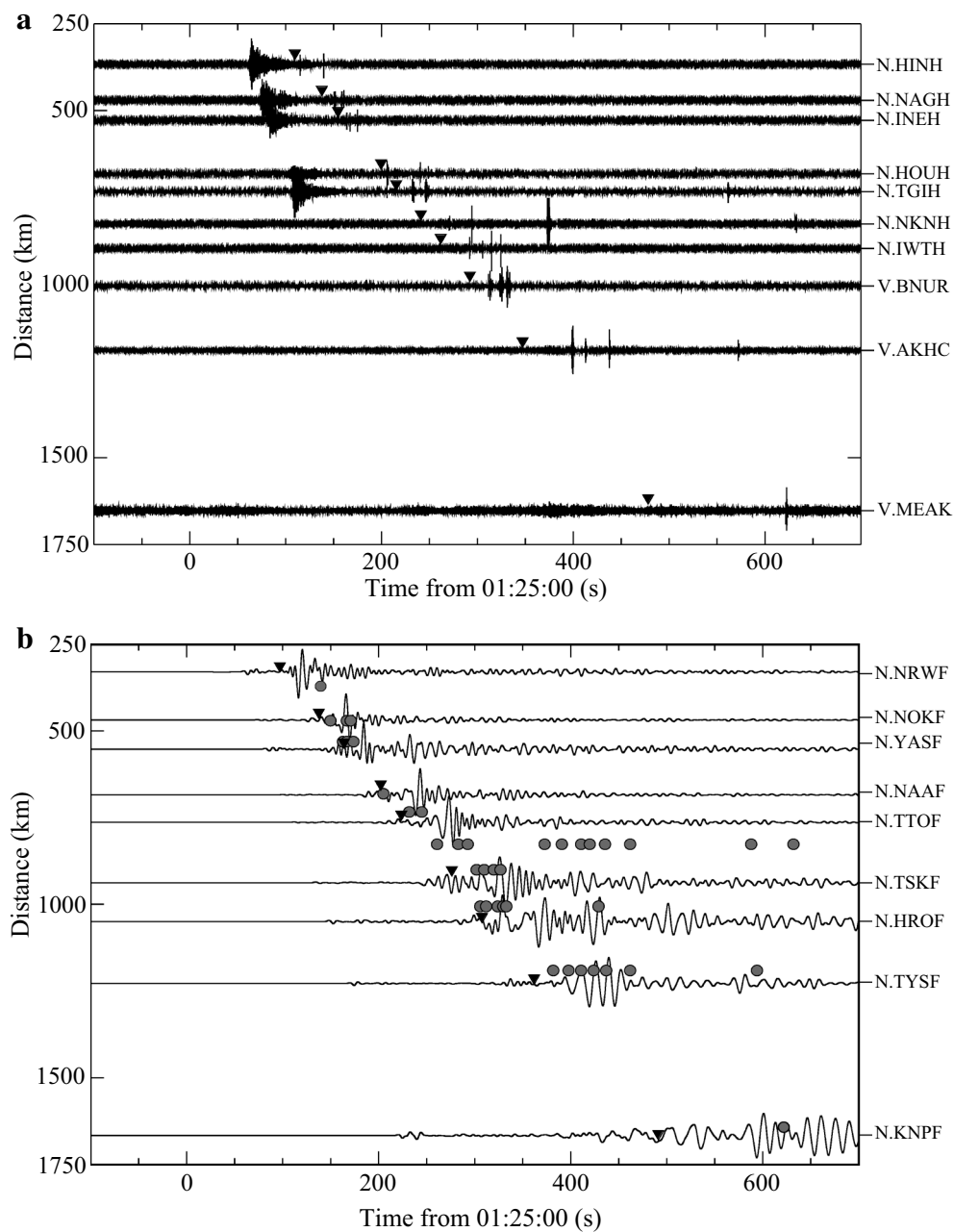
Fig. 2 Remote earthquake triggering during the passage of surface waves. **a** Continuous velocity waveforms observed at Hi-net and JMA stations (vertical components), showing remote triggering due to the Kumamoto earthquake. The waveforms are band-pass-filtered in the frequency range of 10–30 Hz and normalized to the maximum value on each seismogram. They are ordered function of epicentral distance, with distance increasing from up to down. Time is relative to the 01:25:00, on April 16, 2016 (i.e., 5 s before the occurrence time of the Kumamoto earthquake). The name of each recording station is indicated on the *right of the plot*. **b** Low-frequency vertical-component seismograms (0.01–0.2 Hz) observed at F-net stations located closely to the Hi-net stations in (**a**), ordered function of epicentral distance and normalized. The *gray circles* indicate P-wave arrival times of remotely triggered earthquakes, as observed at the Hi-net stations shown in (**a**). *Gray inverted triangles* in both **a** and **b** indicate the arrival of Rayleigh waves, for a phase velocity of 3.5 km/s

We show in Fig. 3c the furthest earthquake triggering from the Kumamoto region, observed in Hokkaido, at an epicentral distance of ~1650 km, close to Akan volcano,

which is one of the most active in Hokkaido. The local triggering (close to the JMA station MEAK: (S-P) time is of ~1 s) correlates with the passage of a relatively large

Enescu *et al. Earth, Planets and Space* (2016) 68:165

Page 6 of 9

Fig. 3 Remote seismicity triggering in Noto Peninsula, Tohoku region and Hokkaido, respectively. **a** Low-frequency (0.01–0.2 Hz) velocity seismograms observed at the Hi-net AMZH station (up to down: vertical, radial and transverse components), in Noto Peninsula, and high-frequency (10–30 Hz), vertical velocity seismogram at TGIH station (Hi-net). The *plot at the bottom* shows the P- and S-wave arrivals of the remotely triggered earthquake at the station TGIH (EW and UD components); **b** Same as in (**a**), but for Tohoku region. The low-frequency and high-frequency recording stations are NSSH (Hi-net) and AKHC (JMA), respectively. **c** Same as in (**a**), but for Hokkaido region. The low-frequency and high-frequency recording stations are ANNH (Hi-net) and MEAK (JMA), respectively. The *bottom plot* in **b** and **c** shows P- and S-wave arrivals on NS and UD components. The reference time in **a**, **b** and **c** is the same as for Fig. 2. The epicentral distances, in km, are also indicated. The names of the stations are written by omitting the "N." and "V." part, for the Hi-net and JMA (volcanic) networks, respectively. The *vertical dotted lines* indicate the window of larger amplitude surface waves

Enescu *et al. Earth, Planets and Space* (2016) 68:165

Page 7 of 9

Rayleigh wave train (as seen on the vertical and radial components at station ANNH).

Maximum shaking peak amplitudes and dynamic triggering levels; triggering mechanisms

We first discuss the peak mainshock surface-wave amplitudes at F-net stations (Fig. 1) located close to areas where triggering was observed after the Kumamoto earthquake. These amplitudes are typically equal or above 0.2 cm/s, with the exception of Hokkaido, where smaller peak amplitudes (of ~0.1 cm/s) have been recorded. Harrington and Brodsky (2006) show that for the case of the 2004 Sumatra earthquake, which produced peak shaking amplitudes in the range 0.25–0.7 cm/s in Japan (their Figure 5), only the largest amplitudes (~0.7 cm/s) were associated with some remotely triggered events (occurred in Kyushu region). Therefore, smaller levels of shaking were capable of triggering earthquakes in Japan in the case of the 2016 Kumamoto mainshock.

We also estimate the peak dynamic stress changes associated with the passage of Rayleigh and Love waves in the triggered regions from the amplitudes of the surface-wave ground velocities (e.g., Peng et al. 2009). Assuming plane wave propagation for teleseismic waves, the peak dynamic stress σ_d is proportional to Gu'/V_{ph} (Jaeger and Cook 1979), where G is the shear modulus, u' is the peak particle velocity, and V_{ph} is the phase velocity. Using a nominal G value of 30 G Pa, $V_{ph} = 4.1$ km/s for the Love waves, and $V_{ph} = 3.5$ km/s for the Rayleigh waves, we estimate dynamic stress change values.

Thus, at a relatively close location (epicentral distance of ~470 km), in Wakayama region (N.NAGH) the maximum dynamic stress changes measured on the vertical, radial and transverse components have rather large values on the order of 91–126 kPa. In Noto Peninsula (Fig. 3a, station AMZH) and in Tohoku region (Fig. 3b, station NSSH), the dynamic stress changes are on the order of 24–56 kPa and 16–33 kPa, respectively. Finally, at the most remote triggering location, in Hokkaido (Fig. 3c, station ANNH), the dynamic stress changes are on the order of 5–11 kPa. These last values are similar to the minimum dynamic stress values, of a few kPa, reported in other studies as capable of triggering earthquakes (e.g., Aiken and Peng 2014). van der Elst and Brodsky (2010) report minimum dynamic stresses that could trigger earthquakes on the order of 0.1 kPa or even lower, using an improved approach. Nevertheless , Japan showed much higher thresholds (order of 90 kPa) (van der Elst and Brodsky 2010), which qualitatively agrees with the results of Harrington and Brodsky (2006). Although the 2011 M9.0 Tohoku-oki earthquake was followed by relatively vigorous remote activation, the reported dynamic triggering thresholds were quite

high (Miyazawa 2011), similar to those reported by van der Elst and Brodsky (2010) for Japan. All these results suggest that the minimum dynamic triggering threshold in Japan, as observed in the current study, is decreased compared to previously reported values. Note that while the estimation of dynamic stresses using surface-wave amplitudes measured at Hi-net stations might lead to some underestimation, the order of these values is robust (Shimojo et al. 2014). Moreover, the smaller amplitudes are much less affected.

We have investigated the predominant surface-wave frequencies that are responsible for the remote triggering after the Kumamoto earthquake and found wave periods of 10–25 s, similar to other cases of dynamic triggering (e.g., Yukutake et al. 2011; Hill and Prejean 2015). We show in the Additional file 1: Figure S3 the amplitude spectra for the surface waves responsible for the triggering in Fig. 3 (the predominant periods are of 10–20 s, in these cases). Note that the passage of surface waves, in this frequency range, was less capable to trigger seismicity in Japan in previous study cases (Harrington and Brodsky 2006), at similar shaking amplitudes.

We have checked the JMA earthquake catalog as well to see whether any significant change in seismicity has been taking place remotely, following the 2016 Kumamoto earthquake. We did not find any evidence for an increase in seismicity using the catalog data. The triggered events we have detected and handpicked (Figs. 2b, 3) on seismograms are very small, with magnitudes of ~1.0, based on a rough estimation. It is therefore reasonable to assume that such small events were not recorded by JMA. Note also that in the majority of cases, the triggering has been observed only during the surface-wave train, with no continuation at later times. From this point of view, we can describe the overall remote seismicity triggering after the Kumamoto earthquake as widespread, but relatively weak.

Since most of the remotely triggered events after the 2016 Kumamoto earthquake have been observed at volcanoes, the excitation of fluids by the passage of the mainshock surface waves might have contributed to receiver fault lubrication, thus facilitating the activation of remote seismicity. More specifically, the passage of mainshock Rayleigh waves might have induced volume changes, thus pressurizing fluids that are active triggering agents in geothermal and volcanic regions (Hill and Prejean 2015). This could be well the case for the activation of seismicity at Akita-Komagatake and Akan volcanoes (Fig. 3b, c, as well as discussion in "Remote events triggered during the passage of Kumamoto earthquake surface waves" section).

The source directivity might be responsible for the relatively large shaking, up to large epicentral distances. Note

Enescu *et al. Earth, Planets and Space* (2016) 68:165

Page 8 of 9

that the rupture along the fault propagated from SW toward NE (Yagi et al. 2016) and most of the seismicity has been triggered along this direction. A similar directivity effect has been observed for the triggering following the 2011 Tohoku-oki earthquake (Miyazawa 2011).

Note also that strike-slip events may radiate more energy than thrust events (Choy and Boatwright 1995) and are much more effective in generating Love waves (Fukao and Abe 1971), in particular. One could speculate that the Love waves, which can induce shearing motion, were the main triggering factor of seismicity in active fault regions, like Noto, Wakayama and Tottori. The occurrence of remotely triggered events in such regions, which are seismically active, may point out that such areas are easier to activate since tectonic stresses there are relatively high, close to some critical threshold value. For the particular case of Noto, the seismicity in the region has mainly thrust-type focal mechanisms; however, some strike-slip motion component is often observed (e.g., the 2007 M6.9 Noto earthquake; Asano and Iwata 2011). The Love waves from the Kumamoto earthquake, arriving from an almost parallel direction to the Noto fault plane (of SW–NE direction, dip angle of 60º—Asano and Iwata 2011), would have a relatively high triggering potential on such faults, at shallow depth (Hill 2012).

After the 2011 Tohoku-oki earthquake, the seismicity all over Japan has been significantly affected. Either static (e.g., Toda et al. 2011; Enescu et al. 2012) or dynamic (e.g., Miyazawa 2011; Yukutake et al. 2011) stress changes were reported being responsible for such seismicity changes. A quick check shows that sites where dynamic triggering has been observed due to the 2016 Kumamoto earthquake were also activated immediately after the 2011 Tohoku-oki earthquake, for a relatively short time (Additional file 1: Figure S2). In many cases, the increase in seismicity in inland regions after the 2011 Tohoku-oki earthquake has been associated with pore pressure changes and fluid excitation, in particular at volcanic or geothermal sites (e.g., Shimojo et al. 2014; Kosuga 2014). Brenguier et al. (2014) showed that volcanic fluids have been pressurized in NE Japan, likely due to the passage of seismic waves from the 2011 Tohoku-oki earthquake. We therefore hypothesize that the triggering conditions might have changed in Japan (NE Japan in particular), after the 2011 Tohoku-oki earthquake, due to the mechanical weakening of a pressurized crust. This could explain the widespread remote triggering observed after the 2016 Kumamoto earthquake, at dynamic stress change levels significantly smaller then reported before for Japan. However, to fully verify this hypothesis, more detailed studies are necessary. The occurrence of other similar large inland earthquakes in the future may help understand whether the "trigger-ability" in Japan has changed due to the 2011 Tohoku-oki earthquake.

Conclusions

We have documented relatively widespread remote triggering of seismicity following the $M_{JMA}7.3$ Kumamoto earthquake, occurred on April 14, 2016, in Kyushu Island, along a strike-slip fault. Our analysis shows clearly that the triggering occurred during the passage of the surface waves from the Kumamoto mainshock. This is the most significant case of remote seismicity activation in Japan, with the exception of the 2011 Tohoku-oki earthquake, which produced as well widespread dynamic triggering (Miyazawa 2011).

The dynamic stresses in the triggered regions range from several kPa to tens of kPa. The threshold dynamic stresses that can trigger seismicity are of a few kPa (e.g., Aiken and Peng 2014); however, larger thresholds have been reported for Japan (e.g., van der Elst and Brodsky 2010). We hypothesize that a change in triggering conditions may have taken place after the 2011 Tohoku-oki earthquake, in particular at volcanic areas in NE Japan.

Since most of the remotely triggered earthquakes have been observed at volcanoes, we suggest that the excitation of fluids may have been the main triggering mechanism. The significant shaking up to relatively large distances, due to a strong directivity effect, may explain the observed spatial distribution of the triggered events.

Additional file

Additional file 1. Additional figures.

Author details

[1] Department of Geophysics, Faculty of Science, Kyoto University, Kita-Shirakawa, Oiwake-cho, Sakyo-ku, Kyoto 606-8502, Japan. [2] Graduate School of Life and Environmental Sciences, University of Tsukuba, Tsukuba, Ibaraki 305-8572, Japan. [3] Faculty of Life and Environmental Sciences, University of Tsukuba, Tsukuba, Ibaraki 305-8572, Japan.

Enescu *et al. Earth, Planets and Space* (2016) 68:165

Page 9 of 9

References

Aiken C, Peng Z (2014) Dynamic triggering of microearthquakes in three geothermal regions of California. J Geophys Res 119:6992–7009. doi:10.1002/2014JB011218

Aiken C, Peng Z, Chao K (2013) Tremors along the Queen Charlotte Margin triggered by large teleseismic earthquakes. Geophys Res Lett 40:829–834. doi:10.1002/grl.50220

Aki A, Richards PG (2002) Quantitative Seismology, 2nd edn. University Science Books, Sausalito

Asano K, Iwata T (2011) Source rupture process of the 2007 Noto Hanto, Japan, earthquake estimated by the joint inversion of strong motion and GPS data. Bull Seismol Soc Am 101:2467–2480

Brenguier F, Campillo M, Takeda T, Aoki Y, Shapiro NM, Briand X, Emoto K, Miyake H (2014) Mapping pressurized volcanic fluids from induced crustal seismic velocity drops. Science 345:80–82. doi:10.1126/science.1254073

Brodsky EE, Karakostas V, Kanamori H (2000) A new observation of dynamically triggered regional seismicity: earthquakes in Greece following the August, 1999, Izmit, Turkey earthquake. Geophys Res Lett 27:2741–2744

Choy GL, Boatwright JL (1995) Global patterns of radiated seismic energy and apparent stress. J Geophys Res 100:18205–18228

Enescu B, Aoi S, Toda S, Suzuki W, Obara K, Shiomi K, Takeda T (2012) Stress perturbations and seismic response associated with the 2011 M9.0 Tohoku-oki earthquake in and around the Tokai seismic gap, central Japan. Geophys Res Lett 39:L00G28. doi:10.1029/2012GL051839

Fukao Y, Abe K (1971) Multi-mode Love waves excited by shallow and deep earthquakes. Bull Earthq Res Inst 49:1–12

Harrington RM, Brodsky EE (2006) The absence of remotely triggered seismicity in Japan. Bull Seismol Soc Am 96:871–878. doi:10.1785/0120050076

Hill DP (2012) Dynamic stresses, Coulomb failure, and remote triggering—corrected. Bull Seismol Soc Am 102:2313–2336. doi:10.1785/0120120085

Hill DP, Prejean SG (2015) Dynamic triggering, chapter 8, Vol 4, "Earthquake Seismology". In: Kanamori H, Schubert G (eds) Treatise on geophysics, 2nd edn. Elsevier, Amsterdam, pp 273–304

Hill DP, Reasenberg PA, Michael A, Arabaz WJ, Beroza G, Brumbaugh D, Brune JN, Castro R, Davis S, dePolo D, Ellsworth WL, Gomberg J, Harmsen S, House L, Jackson SM, Johnston MJS, Jones L, Keller R, Malone S, Munguia L, Nava S, Pechmann JC, Sanford A, Simpson RW, Smith RB, Stark M, Stickney M, Vidal A, Walter S, Wong V, Zollweg J (1993) Seismicity remotely triggered by the magnitude 7.3 Landers, California, earthquake. Science 260:1617–1623

Jaeger JC, Cook NGW (1979) Fundamentals of rock mechanics, 3rd edn. Chapman and Hall, New York

Kosuga M (2014) Seismic activity near the Moriyoshi-zan volcano in Akita Prefecture, northeastern Japan: implications for geofluid migration and a midcrustal geofluid reservoir. Earth Planets Space 66:77. doi:10.1186/1880-5981-66-77

Maeda T, Obara K, Furumura T, Saito T (2011) Interference of long-period seismic wavefield observed by the dense Hi-net array in Japan. J Geophys Res 116:B10303. doi:10.1029/2011JB008464

Manga M, Brodsky E (2006) Seismic triggering of eruptions in the far field: volcanoes and geysers. Annu Rev Earth Planet Sci 34:263–291

Miyazawa M (2011) Propagation of an earthquake triggering front from the 2011 Tohoku-Oki earthquake. Geophys Res Lett 38:L23307. doi:10.1029/2011GL049795

Parsons T, Segou M, Marzocchi W (2014) The global aftershock zone. Tectonohpys 618:1–34. doi:10.1016/j.tecto.2014.01.038

Peng Z, Vidale JE, Wech AG, Nadeau RM, Kreager KC (2009) Remote triggering of tremor along the San Andreas Fault in Central California. J Geophys Res 114:B00A06. doi:10.1029/2008JB006049

Shimojo K, Enescu B, Yagi Y, Takeda T (2014) Fluid-driven seismicity activation in northern Nagano region after the 2011 M9.0 Tohoku-oki earthquake. Geophys Res Lett 41:7524–7531. doi:10.1002/2014GL061763

Toda S, Stein RS, Lin J (2011) Widespread seismicity excitation throughout central Japan following the 2011 M = 9.0 Tohoku earthquake, and its interpretation by Coulomb stress transfer. Geophys Res Lett 38:L00G03. doi:10.1029/2011GL047834

van der Elst NJ, Brodsky EE (2010) Connecting near-field and far-field earthquake triggering to dynamic strain. J Geophys Res 115:B07311. doi:10.1029/2009JB006681

Yagi Y, Okuwaki R, Enescu B, Kasahara A, Miyakawa A, Otsubo M (2016) Rupture process of the 2016 Kumamoto earthquake in relation with the thermal structure around Aso volcano. Earth Planets Space 68:118. doi:10.1186/s40623-016-0492-3

Yukutake Y, Honda R, Harada M, Aketagawa T, Ito H, Yoshida A (2011) Remotely-triggered seismicity in the Hakone volcano following the 2011 off the Pacific coast of Tohoku earthquake. Earth Planets Space 63:737–740. doi:10.5047/eps.2011.05.004